Journal of Molecular Structure 1114 (2016) 21–29

Contents lists available at ScienceDirect

Journal of Molecular Structure

journal homepage: http://www.elsevier.com/locate/molstruc

Syntheses, characterization and antifungal activity of heteroleptic nickel(II) complexes with *N*-alkylsulfonyldithiocarbimates and phosphines

Antonio E.C. Vidigal [a], Mayura M.M. Rubinger [a, *], Marcelo R.L. Oliveira [a], Silvana Guilardi [b], Rafael A.C. Souza [b], Javier Ellena [c], Laércio Zambolim [d]

[a] Departamento de Química, Universidade Federal de Viçosa, Viçosa, MG, CEP 36570-000, Brazil
[b] Instituto de Química, Universidade Federal de Uberlândia, Uberlândia, MG, CEP 39400-902, Brazil
[c] Instituto de Física de São Carlos, Universidade de São Paulo, São Carlos, SP, CEP 13566-590, Brazil
[d] Departamento de Fitopatologia, Universidade Federal de Viçosa, Viçosa, MG, CEP 36570-000, Brazil

ARTICLE INFO

Article history:
Received 22 December 2015
Received in revised form
15 February 2016
Accepted 15 February 2016
Available online 17 February 2016

Keywords:
Dithiocarbimates
Phosphynes
Nickel(II) complexes
Antifungal activity
Crystal structure

ABSTRACT

Four nickel(II) complexes of general formula [Ni($RSO_2N{=}CS_2$)(PPh_3)$_2$] where R = CH_3 (**2a**), CH_3CH_2 (**2b**), $CH_3(CH_2)_3$ (**2c**) and $CH_3(CH_2)_7$ (**2d**) and PPh_3 = triphenylphosphine; and two nickel(II) complexes of general formula [Ni($RSO_2N{=}CS_2$)dppe] where R = $CH_3(CH_2)_3$ (**3c**) and $CH_3(CH_2)_7$ (**3d**) and dppe = 1,2-bis(diphenylphosphine)ethane) were prepared. These new complexes were obtained by the reaction of nickel(II) chloride hexahydrate with potassium *N*-alkylsulfonyldithiocarbimates and the appropriate phosphine using ethanol/water as solvent. The IR, UV–Vis and ^{1}H, ^{13}C and ^{31}P NMR spectra, elemental analysis of Ni and the HR-ESI-MS were consistent with the formation of square planar nickel(II) complexes with mixed ligands. The structures of the compounds **2b** and **2c** were determined by single crystal X-ray diffraction. The compounds are isostructural and crystallize in the space group $P\bar{1}$ of the triclinic system. The activities of the complexes were investigated *in vitro* against *Botrytis cinerea*, *Colletotrichum acutatum* and *Alternaria solani*, fungi species that affect various commercially important plants. All the complexes were active.

1. Introduction

Dithiocarbamates and their complexes are widely used in agriculture. They are multisite contact fungicides that work by protecting the plant surface to prevent infection [1]. Interestingly, these compounds are also used as accelerators of the rubber vulcanization process [2]. Although presenting related structures (Scheme 1), dithiocarbimates are much less common in the literature and have no industrial or commercial applications yet. Aiming to deepen the knowledge on the dithiocarbimates chemistry and applications, we have been investigating the synthesis of dithiocarbimate-metal complexes and their antifungal and vulcanization activities. We have discovered that homoleptic Zn(II), Ni(II) and Sn(IV) complexes with *N*-R-sulfonyldithiocarbimates are active against *Colletotrichum gloeosporioides* and *Botrytis cinerea* [3–6], and also that Zn(II) and Ni(II) complexes with these ligands are good accelerators for the vulcanization of natural rubber [7,8]. Some heteroleptic nickel, palladium and platinum complexes with aromatic sulfonyldithiocarbimates and phosphines have also been prepared [9–12], but no biological studies with these compounds were reported so far.

Here we describe the syntheses and characterization of six new heteroleptic nickel(II) complexes with alkylsulphonyldithiocarbimates and phosphine ligands, and their antifungal activities against *B. cinerea, Colletotrichum acutatum* and *Alternaria solani*.

B. cinerea is responsible for the gray mold disease on more than 200 host plants [13]. *C. acutatum* is an important anthracnose pathogen, also infecting a wide variety of hosts, including vegetables, field and forage crops, fruit trees and ornamentals [14]. The early blight disease caused by *A. solani* has a great destructive power on tomato and potato cultures [15]. *Alternaria* and *Colletotrichum* species are also related to human infections, especially in immunocompromised patients [16].

* Corresponding author.
E-mail address: mayura@ufv.br (M.M.M. Rubinger).

http://dx.doi.org/10.1016/j.molstruc.2016.02.060
0022-2860/

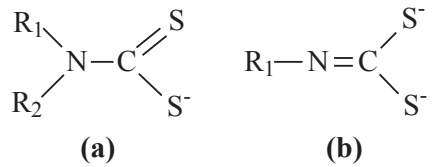

Scheme 1. General formulas of (a) dithiocarbamate and (b) dithiocarbimate anions.

2. Experimental

2.1. Materials and methods

The nickel(II) chloride hexahydrate, triphenylphosphine, carbon disulfide, potassium hydroxide and the solvents were purchased from Vetec and used without further purification. Methanesulfonamide, ethanesulfonyl chloride, butanesulfonyl chloride, octanesulfonyl chloride and 1,2-bis(diphenylphosphine)ethane were purchased from Aldrich. Alkylsulfonamides (except methanesulfonamide) were prepared from the alkylsulfonyl chlorides by their reaction with concentrated ammonia aqueous solution under reflux. The sulfonamides were isolated after extraction with ethyl acetate and solvent evaporation. The *N*-R-sulfonyldithiocarbimate potassium salts dihydrate were prepared in dimethylformamide from the sulfonamides in reaction with carbon disulfide and potassium hydroxide [8,17,18]. High resolution mass spectra were obtained with a Shimatzu LCMS-IT-TOF mass spectrometer from acetonitrile solutions of the compounds. The UV–Vis spectra were recorded with an Agilent 8453 UV–visible spectroscopy system; the solutions of the compounds were prepared in acetonitrile. The IR spectra were recorded with a Perkin Elmer FT-IR 1000 infrared spectrophotometer using CsI pellets. The NMR spectra were obtained at 300 K using a VARIAN 300 MHz spectrometer, from solutions in $CDCl_3$ with TMS as internal standard for the ^1H (300 MHz) and ^{13}C (75 MHz) spectra, or with H_3PO_4 as external standard for the ^{31}P (121 MHz) spectra. Melting points were determined with a MQAPF-302 equipment and are reported without correction. Nickel was analyzed by atomic absorption with a VARIAN AA-200 Spectrometer. For the biological tests, *B. cinerea* and *C. acutatum* were isolated from infected strawberry tissues and incubated for 4 day at 20 °C and 7 day at 25 °C, respectively. *A. solani* was isolated from infected potato and incubated for 7 day at 25 °C. The culture medium PDA (Potato Dextrose Agar) was purchased from Fluka and was previously sterilized in autoclave for 20 min at 120 °C.

2.2. Syntheses

The syntheses were performed according to Scheme 2.

A solution of the appropriate potassium *N*-R-sulfonyldithiocarbimate dihydrate (1.0 mmol) in water (10 mL) was added to a suspension of the phosphine (1.0 mmol of dppe or 2.0 mmol of triphenylphosphine) in ethanol (30 mL). A solution of nickel(II) chloride hexahydrate (1.0 mmol) in water was added to the suspension and the reaction mixture was stirred for 14 h at room temperature. The color of the suspension changed from green to red/orange. The solid products were filtered, washed with distilled water, ethanol and diethyl ether, and dried under reduced pressure for one day. The yields were *ca.* 85%. The data for compounds **3a** and **3b** were in accord with the literature [10]. The data obtained for the new compounds **2a-d** and **3c-d** are as follows.

*[Ni($CH_3SO_2N{=}CS_2$)(PPh_3)$_2$] (**2a**): Anal.* Calc.: Ni, 7.80. Found: 7.58%. HR-ESI-MS $[M+H]^+$ *m/z* Calc.: 752.0573. Found: 752.0636. M.p. with decomposition (°C): 167.6–168.7. UV–Vis λ (nm), [ε_o (L mol^{-1} cm^{-1})]: 198 [65206], 235 [24440], 256 [15511], 318 [11211], 429 [304] and 548 [104]. IR (most important bands) (cm^{-1}): 1457 ν(C=N), 1305 $\nu_{as}(SO_2)$, 1133 $\nu_{sym}(SO_2)$, 924 $\nu_{as}(CS_2)$ and 375 ν(NiS). ^1H NMR (δ): 7.54–7.15 (m, 30H, H2′–H6′), 2.94 (s, 3H, H2). ^{13}C NMR (δ), *J* (Hz): 197.2 (C1), 41.8 (C2), triphenylphosphine signals: 134.3 (t, J_{CP} = 5.3, C2′ and C6′), 130.7 (s, C4′), 129.2 (d, J_{CP} = 45.9, C1′), 128.3 (t, J_{CP} = 4.5, C3′ and C5′). ^{31}P NMR (δ): 34.36 (s).

*[Ni($CH_3CH_2SO_2N{=}CS_2$)(PPh_3)$_2$] (**2b**): Anal.* Calc.: Ni, 7.66. Found: 7.51%. HR-ESI-MS $[M+H]^+$ *m/z* Calc.: 766.0729. Found: 766.0756. M.p. with decomposition (°C): 162.6–163.5. UV–Vis λ (nm), [ε_o (L mol^{-1} cm^{-1})]: 199 [63245], 230 [23091], 261 [14184], 317 [10223], 427 [483] and 553 [132]. IR (most important bands) (cm^{-1}): 1463 ν(C=N), 1304 $\nu_{as}(SO_2)$, 1134 $\nu_{sym}(SO_2)$, 926 $\nu_{as}(CS_2)$ and 372 ν(NiS). ^1H NMR (δ), *J* (Hz): 7.52–7.17 (m, 30H, H2′–H6′), 3.03 (q, 2H, *J* = 7.2, H2), 1.32 (t, 3H, *J* = 7.4, H3). ^{13}C NMR (δ), *J* (Hz): 196.6 (C1), 48.5 (C2), 8.1 (C3), triphenylphosphine signals: 134.3 (t, J_{CP} = 5.3, C2′ and C6′), 130.7 (s, C4′), 129.3 (d, J_{CP} = 45.9, C1′), 128.3 (t, J_{CP} = 4.5, C3′ and C5′). ^{31}P NMR (δ): 34.36 (s).

*[Ni($CH_3(CH_2)_3SO_2N{=}CS_2$)(PPh_3)$_2$] (**2c**): Anal.* Calc.: Ni, 7.39. Found: 7.45%. HR-ESI-MS $[M+H]^+$ *m/z* Calc.: 794.1041. Found: 794.1115. M.p. with decomposition (°C): 159.4–160.8. UV–Vis λ (nm), [ε_o (L mol^{-1} cm^{-1})]: 198 [65425]; 229 [23340]; 259 [14579]; 317 [10490]; 421 [535] and 557 [154]. IR (most important bands) (cm^{-1}): 1465 ν(C=N); 1300 $\nu_{as}(SO_2)$; 1131 $\nu_{sym}(SO_2)$; 925 $\nu_{as}(CS_2)$ and 373 ν(NiS). ^1H NMR (δ), *J* (Hz): 7.51–7.11 (m, 30H, H2′–H6′), 3.01 (t, 2H, *J* = 9, H2), 1.84–1.71 (m, 2H, H3); 1.41–1.29 (m, 2H, H3), 0.86 (t, 3H, *J* = 6, H4). ^{13}C NMR (δ), *J* (Hz): 196.6 (C1), 53.9 (C2), 25.2 (C3), 21.7 (C4), 13.6 (s, C5), triphenylphosphine signals: 137.3 (t, J_{CP} = 6.0, C2′ and C6′), 130.7 (s, C4′), 129.2 (d, J_{CP} = 45.7, C1′), 128.31 (t, J_{CP} = 5.3, C3′ and C5′). ^{31}P NMR (δ): 34.40 (s).

*[Ni($CH_3(CH_2)_7SO_2N{=}CS_2$)(PPh_3)$_2$] (**2d**): Anal.* Calc.: Ni, 6.90. Found: 6.77%. HR-ESI-MS $[M+H]^+$ *m/z* Calc.: 850.1665. Found: 850.1675. M.p. with decomposition (°C): 148.8–150.1. UV–Vis λ (nm), [ε_o (L mol^{-1} cm^{-1})]: 197 [68614], 228 [23983], 259 [14657], 317 [10647], 419 [714] and 555 [325]. IR (most important bands) (cm^{-1}): 1460 ν(C=N), 1309 $\nu_{as}(SO_2)$, 1134 $\nu_{sym}(SO_2)$, 926 $\nu_{as}(CS_2)$ and 378 ν(NiS). ^1H NMR (δ), *J* (Hz): 7.52–7.14 (m, 30H, H2′–H6′), 3.00 (t, 2H, *J* = 9, H2), 1.85–1.74 (m, 2H, H3), 1.41–1.14 (m, 10H, H4–H8), 0.86 (t, 3H, *J* = 6, H9). ^{13}C NMR (δ), *J* (Hz): 196.5 (C1), 54.2 (C2), 31.8 (C3), 29.1 (C4), 29.0 (C5), 28.5 (C6), 23.2 (C7), 22.6 (C8), 14.1 (C9), triphenylphosphine signals: 134.3 (t, J_{CP} = 5.3, C2′ and C6′), 130.7 (s, C4′), 129.2 (d, J_{CP} = 45.7, C1′), 128.2 (t, J_{CP} = 5.3, C3′and C5′). ^{31}P NMR (δ): 34.44(s).

*[Ni($CH_3(CH_2)_3SO_2N{=}CS_2$)dppe] (**3c**): Anal.* Calc.: Ni, 8.78. Found: 8.52%. HR-ESI-MS $[M+H]^+$*m/z* Calc.: 668.0573. Found: 668.0642. M.p. with decomposition (°C): 204.4–206.4. UV–Vis λ (nm), [ε_o (L mol^{-1} cm^{-1})]: 199 [66890], 260 [27664], 308 [25732], 423 [314] and 480 [139]. IR (most important bands) (cm^{-1}): 1479 ν(C=N), 1290 $\nu_{as}(SO_2)$, 1123 $\nu_{sym}(SO_2)$, 920 $\nu_{as}(CS_2)$ and 375 ν(NiS). ^1H NMR (δ), *J* (Hz): 7.74 (s, 8H, H2′ and H6′), 7.56–7.43 (m, 12H, H3′, H4′ and H5′), 3.08 (t, 2H, *J* = 9, H2), 2.36 (d, 4H, J_{HP} = 17, H1″ and H2″), 1.92–1.77 (m, 2H, H3), 1.45–1.30 (m, 2H, H3), 0.88 (t, 3H, *J* = 6, H4). ^{13}C NMR (δ), *J* (Hz): 198.1 (C1), 54.1 (C2), 25.4 (C3), 21.7 (C4), 13.6 (C5), dppe signals: 132.9 (t, J_{CP} = 5.3, C2′ and C6′), 131.8 (s, C4′), 129.3 (t, J_{CP} = 5.2, C3′ and C5′), 128.3 (t, J_{CP} = 22.3, C1′), 25.9 (t, J_{CP} = 23.3, C1″ and C2″). ^{31}P NMR (δ): 58.49 (s).

*[Ni($CH_3(CH_2)_7SO_2N{=}CS_2$)dppe] (**3d**): Anal.* Calc.: Ni, 8.10. Found: 8.47%. HR-ESI-MS $[M+H]^+$ *m/z* Calc.: 724.1197. Found: 724.1251. M.p. with decomposition (°C): 160.6–161.9. UV–Vis λ (nm), [ε_o (L mol^{-1} cm^{-1})]: 199 [70229], 260 [29566], 309 [27276], 423 [605] and 488 [379]. IR (most important bands) (cm^{-1}): 1468 ν(C=N), 1285 $\nu_{as}(SO_2)$, 1126 $\nu_{sym}(SO_2)$, 913 $\nu_{as}(CS_2)$ and 366 ν(NiS). ^1H NMR (δ), *J* (Hz): 7.79–7.67 (m, 8H, H2′ and H6′), 7.56–7.38 (m, 12H, H3′, H4′ and H5′), 3.07 (t, 2H, *J* = 9, H2), 2.36 (d, 4H, J_{HP} = 17, H1″ and H2″), 1.93–1.78 (m, 2H, H3), 1.38–1.19 (m, 10H, H4–H8), 0.85 (t, 3H,

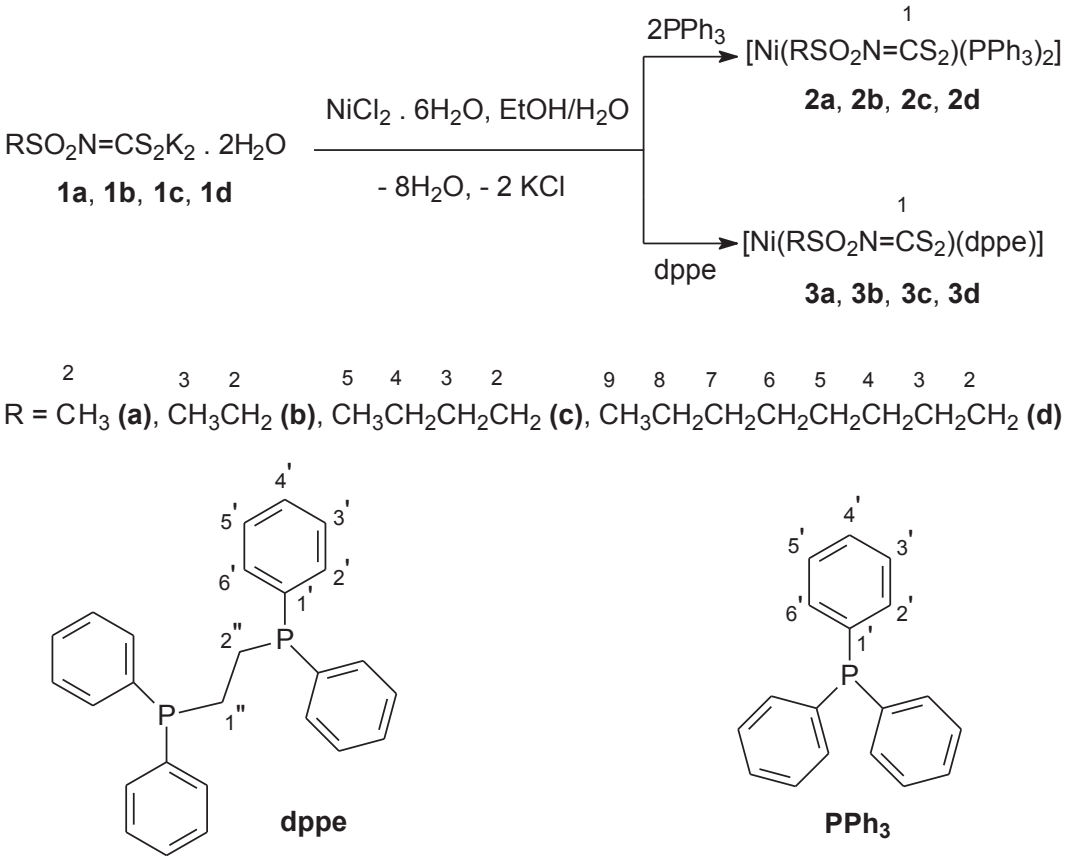

Scheme 2. Syntheses and NMR numbering of the nickel(II) complexes.

$J = 6.7$ Hz, H9). ^{13}C NMR (δ), J (Hz): 197.9 (C1), 54.4 (C2), 31.7 (C3), 29.1 (C4), 29.0 (C5), 28.5 (C6), 23.4 (C7), 22.6 (C8), 14.1 (C9), dppe signals: 132.9 (t, J_{CP} = 5.3, C2′ and C6′), 131.8 (s, C4′), 129.3 (t, $J_{CP} = 5.3$, C3′ and C5′), 128.3 (t, $J_{CP} = 21.8$, C1′), 26.0 (t, $J_{CP} = 23.4$, C1″ and C2″). ^{31}P NMR (δ): 58.28 (s).

2.3. X-ray diffraction studies

Suitable red crystals for X-ray structure analyses were obtained for compounds **2b** and **2c** after slow evaporation of solutions in dichloromethane/ethanol. The single crystal data of the complexes were collected on an Enraf–Nonius Kappa-CCD diffractometer using the graphite-monochromated MoKα radiation (0.71073 Å) at 293.0(2) K. The Bruker AXS Collect software was used for data collection and also for indexing the reflections and determining the unit cell parameters. The collected data were processed using HKL Denzo-Scalepack system of program [19]. Absorption corrections (GAUSSIAN for **2b** and MULTI-SCAN for **2c**) were applied for the complexes using the program SORTAV [20]. The structures were solved by direct methods (SIR-92) and refined (SHELXL-2014) employing full-matrix least-squares on F^2 [21,22]. All H atoms were placed geometrically. The ethyl group in **2b** was disordered over two different orientations with occupancy of 50% each. The SQUEEZE procedure in PLATON was applied for **2b** [23] in order to remove the contribution of the disordered solvent molecules to the intensity of the Bragg reflections. Structural diagrams were drawn using ORTEP-3 [24] and MERCURY [25]. The program WINGX [24] was used to prepare the materials for publication. Crystal data and details on data collection and refinement are summarized in Table 1.

2.4. Biological assay

The antifungal activities were evaluated using the *Poisoned food* technique [3]. Discs of mycelia of the fungi (diameter of 6.25 mm) were placed on the center of Petri dishes containing 15 mL of the culture medium (PDA) homogeneously mixed with the tested compounds at the concentrations of 0.1, 0.2, 0.4, 0.6, 0.8 and 1.0 mmol L^{-1}, plus dimethyl sulfoxide (1% v/v) and Tween 80 (1% v/v). The antibiotic chloramphenicol (0.05 mL) was added to the culture medium for testing with *C. acutatum*. Each treatment consisted of four repetitions and the dishes were incubated at 20 °C for 3 days (*B. cinerea*), 25 °C for 6 days (*C. acutatum*) and 25 °C for 4 days (*A. solani*). The diameter of the fungus colony was measured with a caliper vernier every 24 h from the second day of incubation. The effects of the parent potassium dithiocarbimate salts, triphenylphosphine and dppe were also tested under the same conditions. The control (negative check treatment, four repetitions) was prepared with PDA, dimethylsulfoxide and Tween in the tests with *B. cinerea* and *A. solani*, with the addition of chloramphenicol in the tests with *C. acutatum*. The results were statistically analyzed by nonlinear regression using the concentration versus percent inhibition results. The comparisons of the activities were submitted to analyses of variance and means, and were compared by the Tukey test ($p \leq 0.05$).

3. Results and discussion

The syntheses were performed as shown in Scheme 2. The complexes are stable at room temperature and show red (**2a-d**) and orange (**3a-d**) colors. Their melting temperature ranges were quite narrow although color changes while melting indicated some

Table 1
Crystallographic data and details of diffraction experiments for compounds **2b** and **2c**.

Compound	**2b**	**2c**
Empirical formula	$C_{39}H_{35}NO_2P_2S_3Ni$	$C_{41}H_{39}NO_2P_2S_3Ni$
Formula weight (g mol^{-1})	766.51	794.56
Temperature (K)	293(2)	293(2)
Crystal system	Triclinic	Triclinic
Space group	$P\overline{1}$	$P\overline{1}$
Unit cell dimensions		
a(Å)	11.569(1)	11.704(1)
b(Å)	12.453(2)	12.260(1)
c(Å)	14.050(1)	14.182(1)
α (°)	85.84(1)	86.10(1)
β(°)	72.95(1)	72.39(1)
γ(°)	77.35(1)	77.17(1)
Volume ($Å^3$), Z	1888.1(4), 2	1891.3(2), 2
Calculated density (g cm^{-3})	1.348	1.395
μ (mm^{-1})	0.799	0.800
T_{min}/T_{max}	0.687/0.945	0.784/0.961
F(000)	796	828
Crystal size (mm)	0.306 × 0.189 × 0.049	0.324 × 0.164 × 0.056
θ range (°)	1.676 to 27.521	2.997 to 27.487
Limiting indices	−15,15; −16,16; −18,18	−15,15; −15,15; −18,18
Reflections collected	44330	35588
Independent reflections	8670 [R(int) = 0.0732]	8657 [R(int) = 0.0441]
Goof	1.058	1.068
Data/restraints/parameters	5681/0/442	6104/0/451
R indices [$I > 2\sigma(I)$]	R = 0.0576, wR = 0. 1495	R = 0.0458, wR = 0.1152
R indices (all data)	R = 0.0944, wR = 0.1766	R = 0.0727, wR = 0.1294
Largest diff. peak and hole (e A^{-3})	0.504 and −0.528	0.668 and −0.451

$R_1 = \Sigma\,(||F_o| - |F_c||)/\Sigma|F_o|$; $wR_2 = [\Sigma w(|F_o^2| - |F_c^2|)^2/\Sigma w|F_o^2|^2]^{1/2}$.

degree of decomposition. They are insoluble in water, ethanol, methanol, acetone, hexane, diethyl ether and soluble in dimethylsulfoxide and *N,N*-dimethylformamide. The complexes **2a-d** are also soluble in chloroform, dichloromethane and acetonitrile, while **3a-d** present low solubility in these solvents. The proposed molecular formulas of all compounds could be confirmed from the HR-ESI-MS and atomic absorption spectrometry results. The compounds **3a** and **3b** are described in the literature [10] and their spectroscopic data were in agreement with the published values.

The electronic spectra of the new complexes show a weak band at *ca.* 550 nm (**2a-d**) and *ca.* 480 nm (**3c** and **3d**) due to d−d transitions, indicating a square-planar geometry around the nickel atom. The differences in the position of the d−d bands are consistent with the fact of dppe being a stronger ligand than the triphenylphosphine. The remaining observed bands are due to metal-ligand charge transfer and intraligand transitions [9,10].

The ν(C═N) band (1457−1459 cm^{-1}) in the vibrational spectra of the complexes is shifted to higher wave numbers relative to the spectra of the potassium dithiocarbimates (1282−1301 cm^{-1}), while the CS_2 group vibrations (912−927 cm^{-1}) has an opposite shift (961−970 cm^{-1}, in the spectra of the free ligands [8,17,18]). These results are consistent with a higher character of double bond between the carbon and nitrogen atoms, and a greater character of single bond between the carbon and sulfur atoms in the CS_2 group upon complexation. The medium intensity NiS band was observed in the expected range of 300−400 cm^{-1}.

Comparing the vibrational spectra of the heteroleptic complexes **2a-d** and **3a-d** with those of homoleptic complexes anions of general formula $[Ni(RSO_2N{=}CS_2)_2]^{2-}$, it can be seen that the presence of the phosphines causes an increase in the wavenumbers of the dithiocarbimate ν(C═N) bands. For example, for $[Ni(CH_3(CH_2)_3SO_2N{=}CS_2)(PPh_3)_2]$ (**2c**) the ν(C═N) appears at around 1465 cm^{-1}, while in the spectrum of $(PPh_4)_2[Ni(CH_3(CH_2)_3SO_2N{=}CS_2)_2]$ this band is observed at 1425 cm^{-1} [8]. This difference can be explained by the π acceptor character of the phosphines, causing a drift of electrons from the dithiocarbimate anion to the metal, increasing the double bond character of the C═N bond.

The NMR spectra showed all the expected signals for the compounds and were typical for diamagnetic species, showing narrow and well-defined signals, thus supporting the hypothesis of a square-planar geometry around the nickel atom. The ^1H NMR spectra showed two regions associated with the phosphines (ranging from δ 7.80 to 7.17) and the *N*-alkylsulfonyldithiocarbimates (ranging from δ 3.20 to 0.50) ligands. Their integration curves were consistent with a 2:1 proportion between the triphenylphosphines and the *N*-alkylsulfonyldithiocarbimates, or a 1:1 proportion between the dppe and the *N*-alkylsulfonyldithiocarbimates.

The ^{13}C NMR spectra showed the phosphine carbon signals in the expected range of δ 138 to 127. The *N*-alkylsulfonyldithiocarbimates moieties were responsible for the signals around δ 198 due to the C═N group, and below δ 55 due to the alkyl groups. The chemical shifts of the carbon signals of the *N*-alkylsulfonyldithiocarbimate ligands in the spectra of the complexes do not differ significantly from those observed for the potassium *N*-alkylsulfonyldithiocarbimate salts, except for the positions of the carbon signals of the C═N group. These signals are shifted to higher field if compared with the potassium *N*-alkylsulfonyldithiocarbimate salts and the homoleptic nickel complexes $(PPh_4)_2[Ni(RSO_2N{=}CS_2)_2]$ values [8,17,18]. For example, while the C═N signal appears at δ 196.6 for $[Ni(CH_3CH_2SO_2N{=}CS_2)(PPh_3)_2]$ (**2b**), it is observed at δ 223.8 in the spectrum of $K_2(CH_3CH_2SO_2N{=}CS_2)$ [18], and at δ 212.0 for $(PPh_4)_2[Ni(CH_3CH_2SO_2N{=}CS_2)]$ [8]. These shifts are also consistent with the greater double bond character of the C═N group upon complexation and the extra shielding caused by the drift of electrons from the CS_2 group to the metal, due to the high π acceptor character of the phosphines.

The carbon signals of the triphenylphosphine ligands appear as doublets and triplets in the spectra of the complexes **2a-d**, and the carbon signals of dppe appear as triplet and pseudo-triplet (2:1:2) in the spectra of **3c** and **3d**. The unfolding of these signals occur due to the carbon-phosphorus coupling. This is also consistent with the

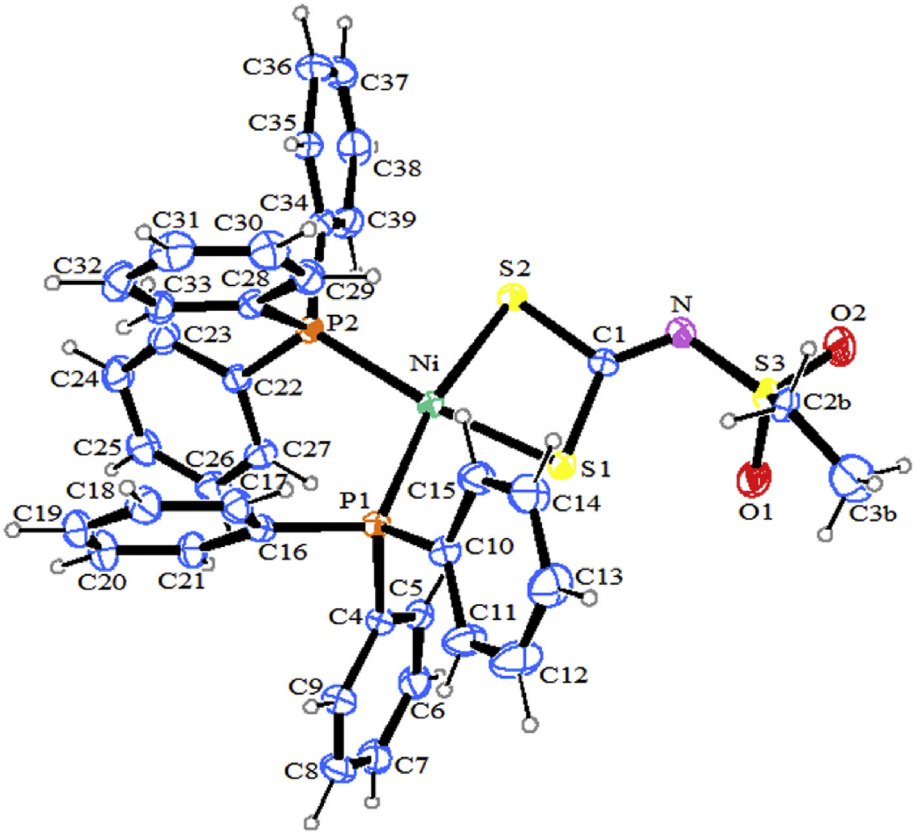

Fig. 1. An ORTEP drawing of **2b** with atom-numbering scheme. Displacement ellipsoids are drawn at the 30% probability level.

square-planar geometry of the complexes, as these multiplicities are commonly observed in the ^{13}C NMR spectra of *cis*-complexes of bis-phosphines with transition metals [26].

The ^{31}P NMR spectra were obtained at a temperature of 300 K.

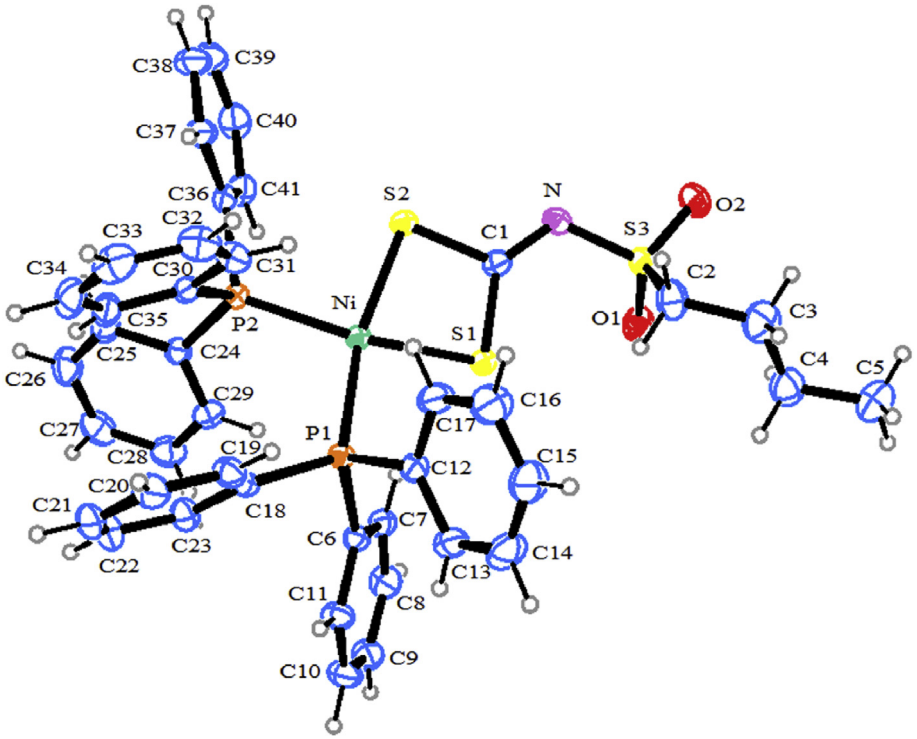

Fig. 2. An ORTEP drawing of **2c** with atom-numbering scheme. Displacement ellipsoids are drawn at the 30% probability level.

Table 2
Selected geometrical parameters for compounds **2b** and **2c**.

Compound	2b	2c
Bond length (Å)		
Ni–S(1)	2.211(1)	2.212(1)
Ni–S(2)	2.193(1)	2.194(1)
Ni–P(1)	2.231(1)	2.232(1)
Ni–P(2)	2.210(1)	2.212(1)
C(1)–S(1)	1.736(4)	1.736(2)
C(1)–S(2)	1.748(4)	1.753(2)
N–C(1)	1.285(5)	1.281(3)
N–S(3)	1.640(3)	1.650(2)
Angles(°)		
S(2)–Ni–P(2)	92.8(1)	92.4(1)
S(1)–Ni–S(2)	78.0(1)	77.9(1)
P(1)–Ni–P(2)	100.1(1)	100.7(1)
S(1)–Ni–P(1)	89.7(1)	90.3(1)
S(1)–C(1)–S(2)	105.4(2)	105.2(1)
N–C(1)–S(1)	132.6(3)	133.1(2)
N–C(1)–S(2)	121.9(3)	121.7(2)
C(1)–N–S(3)	121.5(3)	120.3(2)

Table 3
Hydrogen-bond geometry (Å, °) for compounds **2b** and **2c**.

Donor–H ··· Acceptor	d(D–H)	d(H ··· A)	d(D ··· A)	<(DHA)
*Compound **2b***				
C16–H16···S1	0.96	2.82	3.471(4)	125.9
C38–H38···N^{i}	0.96	2.59	3.483(6)	154.0
*Compound **2c***				
C(4)-H4A ··· O(1)	0.97	2.60	3.235(4)	123.1
C(2)-H2B ··· S(1)	0.97	2.88	3.481(3)	120.8
C(7)-H7 ··· S(1)	0.93	2.88	3.523(3)	127.0
C(16)-H16 ··· O(2)^{ii}	0.93	2.59	3.321(4)	136.5
C(21)-H21 ··· O(1)^{iii}	0.93	2.59	3.462(3)	157.3
C28–H28···O1 ^{iv}	0.93	2.56	3.229(3)	129.3

Symmetry codes: (i) -x, -y, 1-z; (ii) -x, 1-y, -z; (iii) x, y, 1 + z; (iv) 1-x, -y, -z.

signals are shifted to lower field when compared to the free phosphines, that appear at *ca.* δ −5 for triphenylphosphine and −12 for dppe [26,27]. These shifts are caused by the nickel atom, which deshields considerably the phosphorus atoms. Further, a greater electron density on the phosphorus atom of dppe due to the neighbor electron donating methylene group may force the alleviation of excess electron density (from the chelating dppe) to the metal center, in contrast with the triphenylphosphine complexes, where the phosphorus atom is attached to electron withdrawing phenyl groups [28].

Although the phosphorus atoms are not equivalent, no split was observed at 300 K in the ^{31}P NMR spectra. The nonequivalence of the phosphorus atoms becomes evident at lower temperatures. In the spectrum of compound **2d** obtained at 248 K, two doublets are observed at δ 59.63 (J = 39 Hz) and δ 58.74 (J = 39 Hz). The same behavior is observed for other complexes with phosphine ligands where a split of the phosphorus signal becomes evident at *ca.* 240 K [10].

Single crystal X-ray diffraction data confirmed that the nickel atom is coordinated by two sulfur atoms of the dithiocarbimate ligand and by two phosphorus atoms of the triphenylphosphines in the complexes **2b** and **2c** (Figs. 1 and 2). The complexes are isostructural and crystallize in the triclinic space group $P\bar{1}$ with two molecules in the unit cell. Table 2 shows selected geometrical parameters for compounds **2b** and **2c**.

The *cis*-NiS_2P_2 fragment has a distorted square planar geometry due to the small S1–Ni–S2 angle (*ca.* 78°) associated with the bidentate chelation of the dithiocarbimate moiety and a large P–Ni–P angle (*ca.* 100°) due to the steric effect of the triphenylphosphine ligands. The C1–N–S3 fragment of the *N*-R-sulfonyldithiocarbimate ligand and the P_2NiS_2 moiety are coplanar. The Ni–P and Ni–S distances are symmetric as reported for similar compounds [10,11].

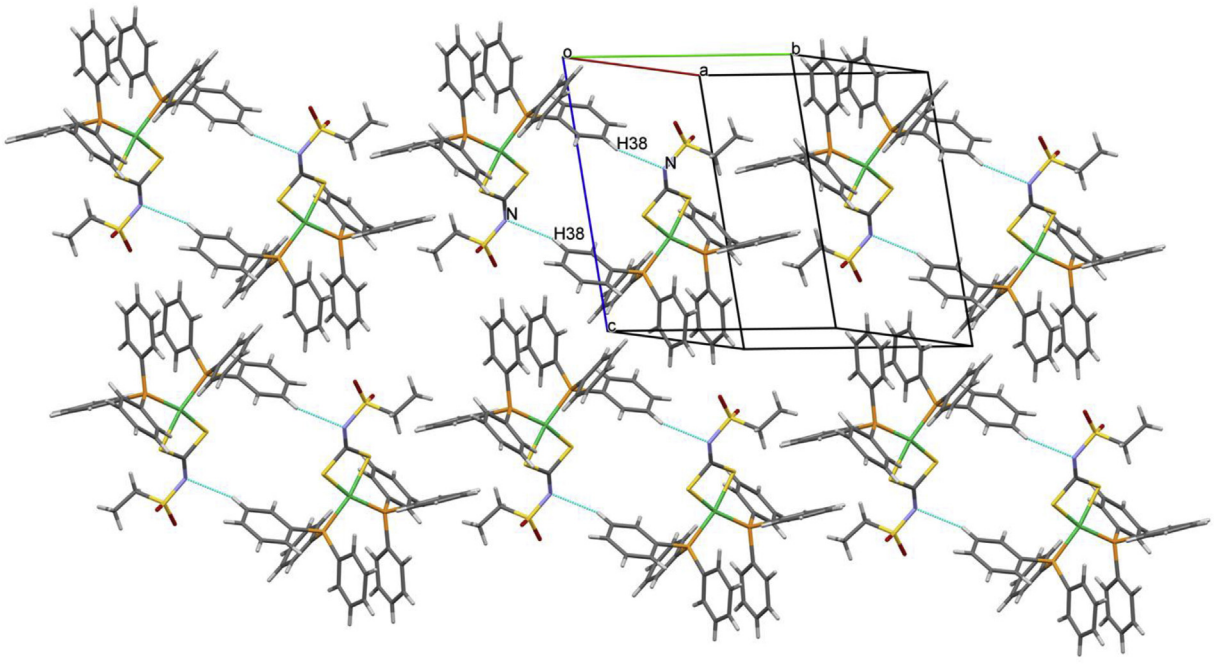

Fig. 3. Packing diagram of **2b**, viewed down the *a* axis. Dashed lines indicate C–H … N intermolecular interactions.

The phosphorus signal was observed at around δ 34 in the spectra of the complexes **2a-d** and at δ 58 in the spectra of **3c** and **3d**. These

In both compounds, the C–S bonds are similar and slightly shorter than typical C–S single bonds (*ca.* 1.81 Å) owing to a partial

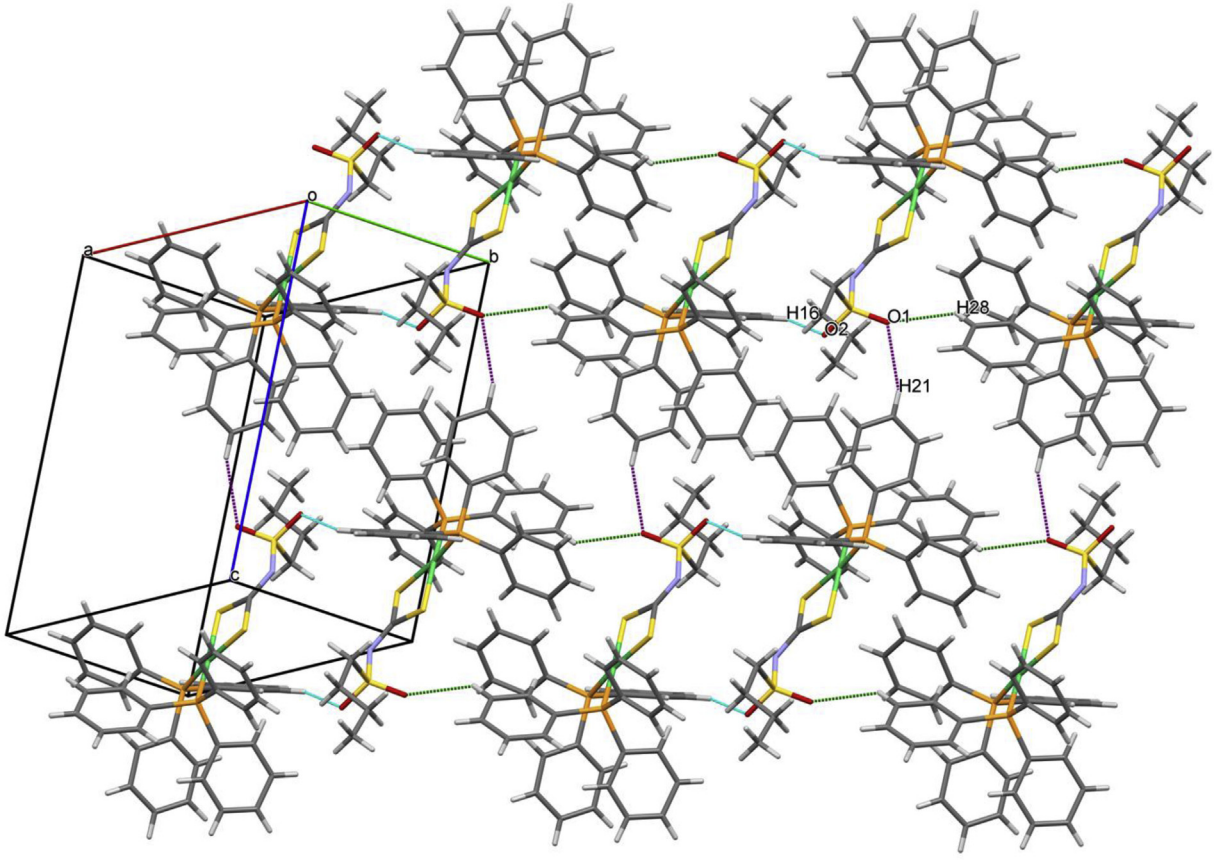

Fig. 4. Packing diagram of **2c**, viewed down the *a* axis. Dashed lines indicate C—H … O intermolecular interactions.

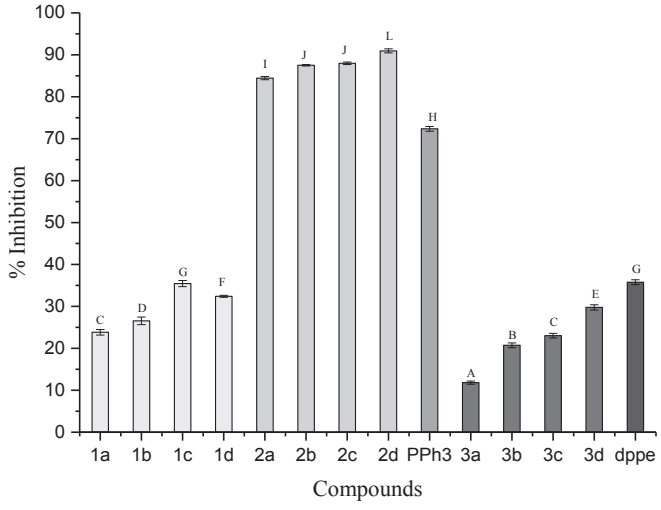

Fig. 5. Percentage of inhibition of *C. acutatum* in the 6th day of incubation in the presence of the potassium *N*-alkylsulfonildithiocarbimates (**1a**-**d**), **PPh$_3$**, **dppe**, and the complexes **2a**-**d** and **3a**-**d**, at 1.0 mmol L^{-1}. Values followed by the same letter do not differ at the 5% level of significance by the Tukey test.

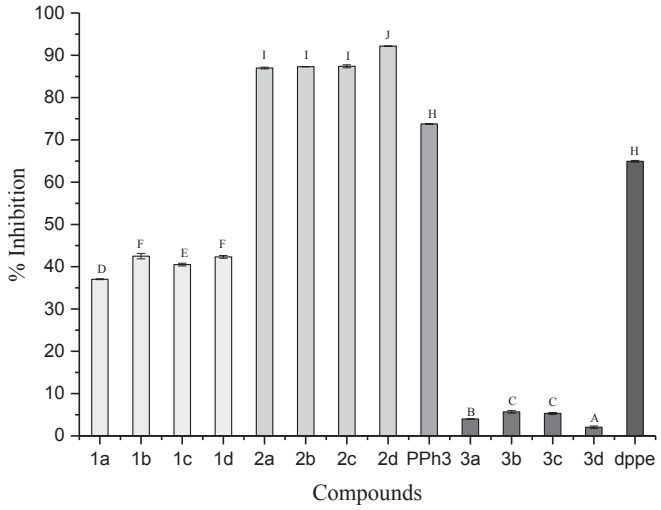

Fig. 6. Percentage of inhibition of *B. cinerea* in the 3rd day of incubation in the presence of the potassium *N*-alkylsulfonildithiocarbimates (**1a**-**d**), **PPh$_3$**, **dppe**, and the complexes **2a**-**d** and **3a**-**d**, at 1.0 mmol L^{-1}. Values followed by the same letter do not differ at the 5% level of significance by the Tukey test.

π-delocalization in the NCS_2 group. The C—N bonds [1.285(5) in **2b** and 1.281(3) Å in **2c**] have a double bond character and are slightly shorter than the ones observed in the potassium dithiocarbimates (approximately 1.35 Å) [29,30]. These results are consistent with the spectroscopic data. Similar behavior is observed for nickel complexes with other dithiocarbimate ligands [9–11].

In both compounds, the bond lengths and angles in the PPh_3 ligands are comparable to those found in similar structures [9,31]. The phosphorus atoms exhibit distorted tetrahedral geometry, the C—P distances and C—P—C angles ranging from 1.812(2) to 1.841(4) Å and 100.5(1) to 110.9(2)°, respectively. The C—C bond lengths in the six phenyl rings varies from 1.354(7) to 1.404(4) Å.

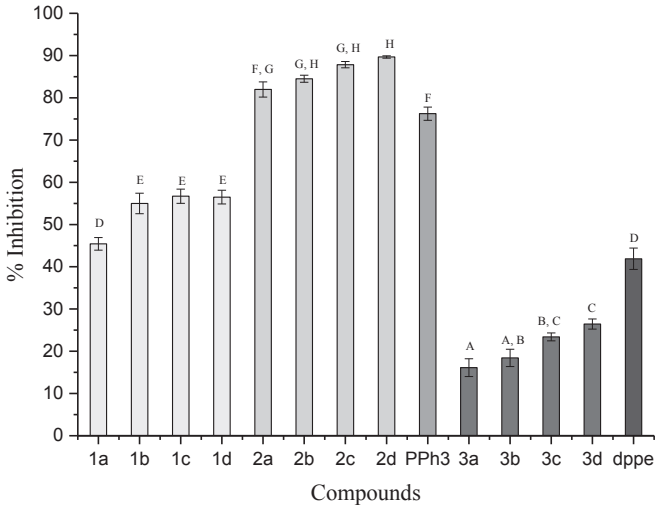

Fig. 7. Percentage of inhibition of *A. solani* in the 4th day of incubation in the presence of the potassium *N*-alkylsulfonildithiocarbimates (**1a-d**), **PPh_3**, **dppe**, and the complexes **2a-d** and **3a-d**, at 1.0 mmol L^{-1}. Values followed by the same letter do not differ at the 5% level of significance by the Tukey test.

The geometric parameters of the interactions in the crystals of compounds **2b** and **2c** are listed in Table 3.

The crystal packing in **2b** shows one C—H ··· S intramolecular interaction and pairs of C—H ··· N hydrogen bonds linking dimmers by an inversion center which generate $R_2^2(18)$ ring motifs along the [110] direction [32]. Van der Waals attractions link the dimmers in a three-dimensional network (Fig. 3).

There are intramolecular contacts (C—H ··· O and C—H ··· S) and three C—H ··· O non classical hydrogen bonds involving O1 and O2 oxygen atoms in the crystal of **2c**. The C16—H16 ··· O2 intermolecular interaction between two molecules related by an inversion center generates a $R_2^2(22)$ ring motif. Each of these molecules also form a second $R_2^2(22)$ ring motif with a neighboring molecule related by another inversion center through a C28—H28 ··· O1 interaction. These motifs are linked by C21—H21 ··· O1 interactions along the *c* axis, giving rise to a supramolecular network (Fig. 4).

The structures show rare C—H···M intramolecular interactions [33–35] as a result of packing effects together with the electronic and steric restrictions of bulky ligands and the d^8 electronic configuration. Interactions characterized by M ··· H distances between 2.3 and 2.9 Å might be important for catalytic applications [35]. In **2b** the H···Ni distance is 2.90 Å and the C—H···Ni angle is 120.4°. Similar, but rather less pronounced, the H···Ni distance in **2c** is 2.96 Å and the C—H···Ni angle is 114.5°.

The analysis of the structure **2b** showed the presence of disordered solvent molecules that could not be reliably modeled and it was thus omitted from the model through the use of SQUEEZE. The void space analysis yielded a volume of 132.7 $Å^3$ with an electron count of 59. This corresponds well to the presence of two ethanol molecules per unit cell.

Table 4
Concentrations of **2a-d** and PPh_3 for 50% inhibition (IC_{50}) of the growth of *Colletotrichum acutatum*, *Botrytis cinerea* and *Alternaria solani*.

Compounds/Fungi	IC_{50} (mmol/L)		
	C. acutatum	*B. cinerea*	*A. solani*
2a	0.52	0.50	0.31
2b	0.46	0.42	0.30
2c	0.40	0.33	0.31
2d	0.41	0.33	0.24
PPh_3	0.53	0.61	0.36

The antifungal activities of the complexes were evaluated against the plant pathogens *B. cinerea*, *C. acutatum* and *A. solani*. The poisoned food methodology was used, where the growth of the pathogen occurs in a culture medium mixed with the compound in test [3]. An estimate of the potential activity is obtained by measuring the diameter of the colony compared to the negative control (white), prepared in the absence of the test substance. In order to allow a complete comparison, the already published complexes **3a** and **3b** [10] were prepared and included in the biological assays. The corresponding potassium *N*-alkylsulfonildithiocarbimates (**1a-d**) and the free phosphines were also included.

The inhibition of the growth of *B. cinerea*, *C. acutatum*, and *A. solani* by all compounds at 1.0 mmol L^{-1} are shown in the Figs. 5–7. The complexes **2a-d** were more active than the free ligands **1a-d** and PPh_3. In contrast, complexes **3a-d** were less active than the potassium *N*-alkylsulfonildithiocarbimates **1a-d** and dppe. Further, it is important to note that due to its low solubility, part of the dppe precipitated in the culture medium. Thus the results for dppe might be underestimated.

The Tukey test at 5% significance was applied to confirm the differences between the inhibition caused by the 14 compounds, and the results are shown in Figs. 5–7. The differences in the length of the carbon chains in the R groups did not interfere appreciably in the activity of the complexes. However, the longer chain of the octyl group did improve the inhibition of *B. cinerea* (Fig. 5) and *C. acutatum* (Fig. 6), according to the Tukey test at 5% level of significance, and the complex **2d** generated the best result of the series, possibly due to a better interaction with the lipophilic cell membrane. Further, the higher activity of the complexes **2a-d** in comparison with the complexes **3a-d** indicated that the mechanism of action might involve the intracellular release of the phosphine ligands from the complexes. This is difficult in the case of **3a-d**, since the nickel(II) forms a chelate with the diphosphine.

To further investigate the activity of compounds **2a-d**, the experiment was repeated in different concentrations in order to obtain the IC_{50} values (Table 4), from nonlinear regression analyses of the dose–response curves. Increasing the carbon chain length causes a slight decrease in the IC_{50} values, confirming that the more lipophilic compounds are the most active ones. These experiments confirmed that the compounds **2a-d** are more active than the free PPh_3.

4. Conclusions

Six new nickel(II) complexes with phosphines and *N*-alkylsulfonyldithiocarbimates were prepared and characterized by high resolution mass spectrometry, elemental analyses for Ni, UV–Vis, IR, ^1H, ^{13}C and ^{31}P NMR. Their structures were further investigated through X-ray diffraction experiments with compounds **2d** and **2c**. The crystallographic data shows that the complexes **2b** and **2c** are isostructural and the coordination about the Ni atom resulted in a distorted square planar geometry. The spectroscopic and X-ray data for **2b** and **2c** show an interesting relation with the data for the homoleptic complexes $[Ni(RSO_2N{=}CS_2)_2]^{2-}$. The C—N bond lengths in **2b** and **2C** are shorter than those in the homoleptic complexes [8]. The wavenumbers for the νCN band in the IR spectra of **2a-d** are greater than those in the spectra of the homoleptic anionic complexes. These bands are observed in even smaller wavenumbers in the spectra of the parent potassium dithiocarbimates [8,17,18]. The NMR spectra show that the carbon atoms of the dithiocarbimate group of **2a-d** are more shielded than those of the anionic complexes and the parent ligands. These facts are in accord with an increase of the CN double bond character in the heteroleptic complexes.

The *N*-alkylsulfonyldithiocarbimate-nickel(II) complexes containing triphenylphosphine (**2a-d**) inhibited the growth of *B. cinerea*, *C. acutatum* and *A. solani* while the complexes with dppe (**3a-d**) were much less active. These results indicated that the mode of action of the complexes might include the intracellular release of the phosphines. An increased activity of the more lipophilic compounds containing the longer dithiocarbimate aliphatic chain (R with 8 carbon atoms), suggested that the stronger interaction with the cell membrane is also important for the activity of these complexes.

Acknowledgments

We are grateful to the Conselho Nacional de Desenvolvimento Científico e Tecnológico (CNPq), Coordenação de Aperfeiçoamento de Pessoal de Nível Superior (CAPES) and Fundação de Amparo à Pesquisa do Estado de Minas Gerais (FAPEMIG) for students' grants and financial support.

Supplementary material

CCDC 1441014 and 1441022 contains the supplementary crystallographic data for **2b** and **2c**, respectively. These data can be obtained free of charge from The Cambridge Crystallographic Data Centre via www.ccdc.cam.ac.uk/data_request/cif.

Appendix A. Supplementary data

Supplementary data related to this article can be found at http://dx.doi.org/10.1016/j.molstruc.2016.02.060.

References

[1] G. Hogarth, P. J, Prog. Inorg. Chem. 53 (2005) 71.
[2] P.J. Nieuwenhuizen, A. Ehlers, J.G. Haasnoot, S.R. Janse, J. Reedijk, E.J. Baerends, J. Am. Chem. Soc. 121 (1999) 163.
[3] L.C. Alves, M.M.M. Rubinger, R.H. Lindemann, G.J. Perpétuo, J. Janczak, L.D.L. Miranda, L. Zambolim, M.R.L. Oliveira, J. Inorg. Biochem. 103 (2009) 1045.
[4] R.S. Amim, M.R.L. Oliveira, J. Janczak, M.M.M. Rubinger, L.M.M. Vieira, L.C. Alves, L. Zambolim, Polyhedron 30 (2011) 683.
[5] L.C. Dias, M.M.M. Rubinger, J.P. Barolli, J.D. Ardisson, I.C. Mendes, G.M. De Lima, L. Zambolim, M.R.L. Oliveira, Polyhedron 47 (2012) 30.
[6] A.A. Oliveira, M.R.L. Oliveira, M.M.M. Rubinger, D.C. Rezende, L. Zambolim, Quím. Nova 38 (2015) 757.
[7] L.M.G. Cunha, M.M.M. Rubinger, M.R.L. Oliveira, E.C. Tavares, J.R. Sabino, E.B.A.V. Pacheco, L.L.Y. Visconte, Inorg. Chim. Acta 383 (2012) 194.
[8] L.M.G. Cunha, M.M.M. Rubinger, J.R. Sabino, L.L.Y. Visconte, M.R.L. Oliveira, Polyhedron 29 (2010) 2278.
[9] M.R.L. Oliveira, H.P. Vieira, G.J. Perpétuo, J. Janczak, V.M. De Bellis, Polyhedron 21 (2002) 2243.
[10] M.R.L. Oliveira, J.A. Amim Jr., I.A. Soares, V.M. De Bellis, C.A. Simone, C. Novais, S. Guilardi, Polyhedron 27 (2008) 727.
[11] M.R.L. Oliveira, E.F. Franca, C. Novais, S. Guilardi, I. Machado Jr., J. Ellena, J.A. Amim Jr., V.M. De Bellis, M.M.M. Rubinger, Inorg. Chim. Acta 376 (2011) 238.
[12] N. Singh, B. Singh, K. Thapliyal, M.G.B. Drew, Inorg. Chim. Acta 363 (2010) 3589.
[13] (a) Y. Elad, B. Williamson, P. Tudzynski, N. Delen, Botrytis - Biology, Pathology and Control, Springer, Dordrecht, 2004, pp. 1–8;
(b) M. Choquer, E. Fournier, C. Kunz, C. Levis, J.M. Pradier, A. Simon, M. Viaud, Microbiol. Lett. 277 (2007), 1; M. Leroch, C. Plesken, R. W. S. Weber, F. Kauff, G. Scalliet, M. Hahna, Appl. Environ. Microbiol. 79 (2013) 159.
[14] (a) B.S.G. Paredes, F.R. Muñoz, Crop Prot. 21 (2002) 11;
(b) S. Freeman, F. Nizani, S. Dotan, S. Even, T. Sando, Plant Dis. 81 (1997) 749.
[15] (a) R. Chaerani, R.E. Voorrips, J. Gen. Plant Pathol. 72 (2006) 335;
(b) A. Horsfield, T. Wicks, K. Davies, D. Wilson, S. Paton, Australas. Plant Pathol. 39 (2010) 368.
[16] A.J. De Lucca, Rev. Iberoam. Micol. 24 (2007) 3.
[17] M.R.L. Oliveira, V.M. De Bellis, Trans. Metal. Chem. 24 (1999) 127.
[18] E.F. Franca, M.R.L. Oliveira, S. Guilardi, R.P. Andrade, R.H. Lindemann, J.A. Amim Jr., J. Ellena, V.M. De Bellis, M.M.M. Rubinger, Polyhedron 25 (2006) 2119.
[19] Z. Otwinowski, W. Minor, in: C.W. Carter Jr., R.M. Sweet (Eds.), Methods in Enzymology, vol. 276, Academic Press, New York, 1997, p. 307.
[20] A.L. Spek, Acta Cryst. D. 65 (2009) 148.
[21] A. Altomare, G. Cascarano, C. Giacovazzo, A. Guagliardi, J. Appl. Cryst. 27 (1994) 435.
[22] G.M. Sheldrick, SHELXL2014, University of Gottingen, Germany, 2014.
[23] R.H. Blessing, Acta Cryst. A 51 (1995) 33.
[24] L. Farrugia, J. Appl. Cryst. 45 (2012) 849.
[25] F. Macrae, P.R. Edgington, P. McCabe, E. Pidcock, G.P. Shields, R. Taylor, M. Towler, J. van de Streek, J. Appl, Cryst 39 (2006) 453.
[26] B.A. Prakasam, K. Ramalingan, M. Saravanan, G. Bocelli, A. Cantoni, Polyhedron 23 (2004) 77.
[27] J.A.S. Bonfim, F.P. De Souza, C.A.L. Filgueiras, A.G. De Souza, M.T.P. Gambardella, Polyhedron 22 (2003) 1567.
[28] B.A. Prakasam, K. Ramalingan, G. Bocelli, A. Cantoni, Bull. Chem. Soc. Jpn. 79 (2006) 113.
[29] R.S. Amim, M.R.L. Oliveira, G.J. Perpétuo, J. Janczak, L.D.L. Miranda, M.M.M. Rubinger, Polyhedron 27 (2008) 1891.
[30] H.U. Hummel, U. Korn, Z. Naturforsch 44B (1989) 24.
[31] Z. Trávníček, P. Starha, R. Pastorek, J. Mol. Struct. 1049 (2013) 22.
[32] M. Etter, Acc. Chem. Res. 23 (1990) 120.
[33] N. Singh, B. Singh, K. Thapliyal, M.G.B. Drew, Inorg. Chim. Acta 363 (2010) 3589.
[34] N. Singh, B. Singh, S.K. Singh, M.G.B. Drew, Inorg. Chem. Commun. 13 (2010) 1451.
[35] H.V. Huynh, L.R. Wong, P.S. Ng, Organometallics 27 (2008) 2231.